Proceedings of the 2007 American Control Conference
Marriott Marquis Hotel at Times Square
New York City, USA, July 11-13, 2007

Model Predictive Control of Magnetic Automotive Actuators

Stefano Di Cairano†, Alberto Bemporad†, Ilya Kolmanovsky‡ and Davor Hrovat‡

Abstract— **Magnetically actuated mass-spring-damper systems are common in automotive systems as components of various actuation mechanisms. They are characterized by nonlinear dynamics, tight performance specifications and physical constraints. Due to these reasons, model predictive control (MPC) is an appealing control framework for such systems. In this paper we describe different MPC approaches to control the magnetically actuated mass-spring-damper system. The MPC controller based on the complete system model achieves very good performance, yet it may be too complex to be implemented in standard automotive microcontrollers. Hence, we consider the possibility of decoupling the electromagnetic subsystem from the mechanical subsystem, assuming that the electromagnetic dynamics, controlled by an inner-loop controller, are much faster than the mechanical dynamics. Based on a previous feasibility study, we implement a control architecture in which the MPC optimizes only the dynamics of the mechanical subsystem, and we test it in closed-loop simulations with the nonlinear system. The resulting control system achieves lower performance, but it is simple enough to be implemented in an automotive microcontroller.**

I. Introduction

During the last few years major advances in automotive applications have been enabled by "smart" electronic devices that monitor and control the mechanical components. Cars have become complex systems in which electronic and mechanical subsystems are tightly connected and interact to achieve optimal performance. Automotive actuators, in particular, have become examples of such *mechatronic* systems [1]–[3]. Their dynamics can be very nonlinear and there are tight operating requirements on their precision, power consumption and performance.

The model predictive control (MPC) [4], [5] provides an attractive approach for *systematic* design and deployment of controllers to meet stringent performance requirements and the physical constraints in such automotive actuation systems. The solution of the optimization problem can be pre-computed off-line obtaining an explicit form of the model predictive controller [6], that allows the application of MPC even in the case of stringent computing time and hardware cost requirements.

In this paper we consider a magnetically actuated mass-spring-damper system with input and state constraints, which embodies many of the challenges encountered in controlling real automotive actuators based on electromagnetic technology [1]–[3]. In this system the mechanical mass-spring-damper subsystem interacts with an electromagnetic subsystem, which provides the force for controlling the mechanical subsystem. The mass position has to track as fast as possible an external reference with a small control effort. Many different constraints must be enforced on both the electromagnetic and the mechanical subsystems. In particular, it is assumed that the electromagnet can only attract but not repel the mass, that the mass is moving within a limited space, that the velocity must be bounded, and that the control input is limited.

In a recent work [7], the authors have analyzed the feasibility of applying MPC techniques, supposing that an inner-outer control architecture can be implemented. In this approach, called *decoupled MPC*, the MPC algorithm uses a prediction model based on the mechanical subsystem only, and generates a force profile that optimizes the tracking of the external reference. An inner-loop controller is supposed to be able to provide such a force by acting on the voltage of the power electronics. The MPC does not take into account the current dynamics and, as a consequence, it cannot optimize the behavior of the entire system, nor enforce constraints on the voltage.

This paper extends the previous work in two main directions. After presenting the full electromechanical system model and the operating constraints in Section II, an MPC controller based on the complete system model is presented in Section III. Such a controller exploits for prediction an approximated hybrid system model of the complete dynamics and it is able to optimize both, the electrical and the mechanical subsystems. This approach achieves good performance, however, it may be too complex to implement in standard automotive microcontrollers. Thus, the second contribution of this paper is the implementation of the controller architecture proposed in [7], and the validation of the controller in closed-loop with the nonlinear dynamics, in Section IV. Finally, the key conclusions are summarized in Section V.

II. Physical Model and Constraints

The magnetically actuated mass-spring-damper system, with the schematics shown in Figure 1, is a heterogenous system composed of a mechanical subsystem and of an electromagnetic subsystem which influence each other. The

Work (partially) done in the framework of the HYCON Network of Excellence, contract number FP6-IST-511368

† S. Di Cairano and A. Bemporad are with Dipartimento di Ingegneria dell'Informazione, Università di Siena, Italy dicairano,bemporad@dii.unisi.it

‡ I. Kolmanovsky and D. Hrovat are with Ford Motor Company, Dearborn, Michigan, USA. ikolmano,dhrovat@ford.com

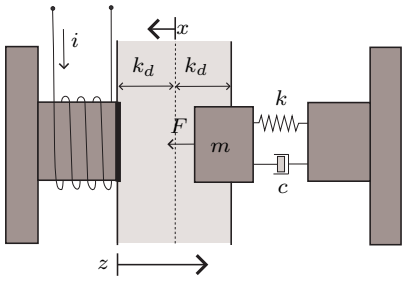

Fig. 1. The schematics of a magnetically actuated mass spring damper system.

equations that define the complete system are

$$m\ddot{x} = F - c\dot{x} - kx, \tag{1a}$$
$$V = Ri + \dot{\lambda}, \tag{1b}$$
$$\lambda = \frac{2k_a i}{k_b + z}, \tag{1c}$$
$$F = \frac{k_a i^2}{(z+k_b)^2} = \frac{\lambda^2}{4k_a}, \tag{1d}$$
$$z = k_d - x. \tag{1e}$$

Equation (1a) represents the dynamics of the mass under the effects of an external force F, of a spring with stiffness k, and of a damper with coefficient c. Equation (1b) represents a resistive circuit with resistance R, in which the effects of magnetic flux variations are considered. The relation between magnetic flux (λ) and current (i) is defined by (1c), where k_a, k_b are constants, while Equation (1d) defines the force either as a function of the current or as a function of the magnetic flux. Equation (1e) defines the relation between position coordinates in the mechanical (x) and in the electromagnetic (z) subsystem. The first has the origin at the neutral position of the spring, while the second at the position at which the mass is in contact with the coil. Moreover, since x takes its maximum value at the contact position, and $k_d = 4{\cdot}10^{-3}$ [m] is the distance between the contact position and the spring neutral position, $z \geq 0$, and if i is bounded, the force is always bounded. The physical model (1), expressed as a dynamical system by taking λ, x, $\dot{x}$ as state variables, is

$$\ddot{x} = \frac{1}{4k_a m}\lambda^2 - \frac{k}{m}x - \frac{c}{m}\dot{x}, \tag{2a}$$
$$\dot{\lambda} = -\frac{R(k_b+k_d)}{2k_a}\lambda + \frac{R}{2k_a}\lambda x + V, \tag{2b}$$

which is clearly nonlinear.

Such a system is subject to several constraints related to physical limits and performance. The position constraint

$$-k_d \leq x \leq k_d \quad [\text{m}] \tag{3}$$

enforces the physical limits of the mass movement, avoiding the mass penetration into the coil or into the stop on the other end. The "soft landing" constraint

$$-\bar{v} + Gx \leq \dot{x} \leq \bar{v} - Gx \quad [\text{m/s}], \tag{4}$$

where $\bar{v}$ and G are constants, is enforced to reduce the noise and wear associated with high velocity collisions due to external disturbances, and to reduce the noise in the electromagnetic subsystem, caused by rapid movements of the mass near the coil. For the mass-spring-damper system we consider here, $\bar{v}$ and G are chosen so that for $x = 0$ mm, $\dot{x} \in [-10.2, 10.2]$ m/s, i.e., the constraint is essentially inactive, while for $x = 4$ mm, $\dot{x} \in [-0.2, 0.2]$ m/s, i.e., the constraint is quite tight and difficult to meet. The current in the circuit must be positive and, as a consequence of (1d), the magnetic force is able to only attract the mass so that

$$i \geq 0 \quad [\text{A}] \tag{5a}$$
$$F \geq 0 \quad [\text{N}] \tag{5b}$$

A constraint on the maximum voltage is considered

$$0 \leq V \leq V_{\max} \ [\text{V}], \tag{6}$$

enforcing the physical limits and the safety of the electrical circuit.

A. Hybridization of nonlinear functions

Optimal control problems for constrained nonlinear systems are hard to solve, because they are in general nonconvex. A common strategy is to find an approximation of the system dynamics. For highly nonlinear dynamics a linear approximation may not be satisfactorily, while it is often possible to find an adequate piecewise linear approximation, resulting in a piecewise affine (PWA) system [8]. In order to design a MPC controller for a nonlinear system, the following approach is applied: (1) The nonlinear dynamics are piecewise linearized, (2) the PWA system is transformed into an equivalent mixed logical dynamical (MLD) system [9], (3) the MLD is used as a prediction model for the hybrid MPC algorithm which is solved by mixed-integer programming (MIP). The universal approximation property of PWA systems [8] ensures that a satisfactory piecewise affine approximating model will eventually be found.

We consider here the simple case of hybridization of one-dimensional functions. Let $g : \mathbb{R} \to \mathbb{R}$ be a nonlinear function, we approximate $g(\cdot)$ by a (continuous) piecewise affine function $f(\chi) = r_i\chi + q_i$, if $\chi \in [\bar{\chi}_i, \bar{\chi}_{i+1})$, $i = 0 \dots \ell - 1$, where $\bar{\chi}_i < \bar{\chi}_{i+1}$ and $\{\bar{\chi}_i\}_{i=1}^{\ell-1}$ are the function breakpoints. Next, we introduce $\ell-1$ binary variables $\delta_1, \dots \delta_{\ell-1} \in \{0,1\}$ defined by the logical conditions

$$[\delta_i = 1] \leftrightarrow [\chi \leq \bar{\chi}_i], \quad i = 1, \dots, \ell - 1, \tag{7}$$

and $\ell - 1$ continuous variables $z_1, \dots, z_{\ell-1} \in \mathbb{R}$ defined by

$$z_i = \begin{cases} (r_{i-1} - r_i)\chi + (q_{i-1} - q_i) & \text{if } \delta_i = 1 \\ 0 & \text{otherwise} \end{cases} \quad i = 1, \dots \ell - 2, \tag{8a}$$
$$z_{\ell-1} = \begin{cases} r_{\ell-2}\chi + q_{\ell-2} & \text{if } \delta_{\ell-1} = 1 \\ r_{\ell-1}\chi + q_{\ell-1} & \text{otherwise} \end{cases} \tag{8b}$$

Then, the piecewise affine approximation of $g(\chi)$ is

$$f(\chi) = \sum_{i=1}^{\ell-1} z_i. \tag{9}$$

Equations (7), (8), and (9), together with other linear equations that defines the system, can be modelled in HYSDEL [10] and automatically translated by the Hybrid Toolbox [11] into the MLD form [12]

$$x(k+1) = Ax(k) + B_1u(k) + B_2\delta(k) + B_3z(k), \quad (10a)$$
$$y(k) = Cx(k) + D_1u(k) + D_2\delta(k) + D_3z(k), \quad (10b)$$
$$E_2\delta(k) + E_3z(k) \leq E_1u(k) + E_4x(k) + E_5. \quad (10c)$$

The additional discrete variables in (7) are the δ vector, while the additional continuous variables in (8) are the z vector. Equation (9) is embedded either in (10a) or in (10c), depending if it is static or dynamic, respectively. Once the system dynamics has been expressed in the MLD form, one can use it to formulate optimal control problem as mixed-integer programming problems [13].

B. Performance evaluation and complexity assessment

For performance evaluation we use the cumulative squared tracking error $\mathcal{E} = \sum_{k=0}^{N_{\text{steps}}}(x(k) - r(k))^2$, where N_{steps} is the number of simulation steps, x is the mass position and r is the external reference, both expressed in mm. The simulations duration is 0.125 s, with a sampling period $T_s = 0.5$ ms, hence $N_{\text{steps}} = 250$. While considering automotive actuators with stringent hardware and timing constraint, the explicit solution of the MPC must be considered for controller complexity evaluation. While the performance of the explicit MPC is identical to the one of the implicit MPC, the explicit controller is pre-computed offline and stored in a lookup table as a set of PWA controllers. A good measure of the explicit controller complexity is the number of regions that constitute the PWA controller, since this number relates to the storage space required required by the controller, and to the number of operations to be performed at each time step.

III. COUPLED MODEL PREDICTIVE CONTROL

The MPC strategy is an optimization-based closed-loop control strategy. Given the measured or estimated state $x(t)$ at time t, a finite horizon constrained optimal control problem is solved obtaining the optimal input profile $U^* = \{u_0^*, u_1^*, \dots u_{N-1}^*\}$. The control input $u(t) = u_0^*$ is applied to the system. At $t+1$, the system state is measured/estimated again and a new optimization problem is solved. MPC schemes differ depending on the system model which is used in the optimal control problem. In the case of a linear system, the optimization problem is a linear program (LP) or a quadratic program (QP), depending on the cost function used. In case of a hybrid system, in which some variables are integer-valued, the optimization problem is a mixed-integer program (MIP) [13].

A. System model

The nonlinear dynamics (2) cannot be used as prediction model for linear/hybrid MPC. We apply the approach of Section II-A to find a piecewise affine approximation of (2).

To this end, consider (2b) and the following change of variables, $\Lambda = \ln \frac{\lambda}{\lambda_0}$, where $\lambda_0 = 1$ [V·s] is used to make the argument of the logarithm non-dimensional. Since $\dot{\Lambda} = \lambda^{-1}\dot{\lambda}$, Equation (2b) becomes

$$\dot{\Lambda} = \frac{R}{2k_a}x + u - \frac{R(k_b + k_d)}{2k_a}, \quad (11)$$

where $u = \frac{V}{\lambda} = \frac{V}{\lambda_0 e^{\Lambda}}$ [s^{-1}] is the input. Thus, taking x and Λ as state variables, system (1) is described by

$$\ddot{x} = -\frac{c}{m}\dot{x} - \frac{k}{m}x + \frac{F}{m}, \quad (12a)$$
$$\dot{\Lambda} = \frac{R}{2k_a}x + u - \frac{R(k_b + k_d)}{2k_a}, \quad (12b)$$
$$F = \frac{\lambda_0^2 e^{2\Lambda}}{4k_a}, \quad (12c)$$
$$u = \frac{V}{\lambda_0 e^{\Lambda}} \leq \frac{V_{\max}}{\lambda_0 e^{\Lambda}}, \quad (12d)$$

which consists of two affine dynamical equations, modelling the mechanical and electromagnetic subsystems, respectively, and of two nonlinear static equations that act as interfaces. In order to obtain a piecewise affine model of such a system, a piecewise affine approximation of static equations (12c), (12d) as functions of Λ is needed. Equation (12d) enforces constraint (6) where $V_{\max} = 350$ V, and results in a piecewise affine constraint on u.

Remark 1: From a mathematical point of view the nonlinear change of variables $\Lambda = \ln \frac{\lambda}{\lambda_0}$ is valid only in the interval $\lambda \in (0, \infty)$. Constraint (5a) enforces $i \geq 0$, so that we have to discuss only the case $i = 0$. Such an error can be considered as a modelling error, since model (12) is used only for prediction by the MPC controller, and it can be arbitrarily small by leaving Λ unbounded from below. However, in order to maintain the possibility of having a force exactly null, in the piecewise linearization we can impose $F = 0$ for $\Lambda \leq \hat{\Lambda}$, where $\hat{\Lambda}$ is a negative number. As a consequence the modelling error occurs for $0 < \lambda \leq \lambda_0 e^{\hat{\Lambda}}$, while for $\lambda = 0$ the approximation is exact. ■

First a discrete-time version of (12a), (12b) with sampling period $T_s = 0.5$ ms is obtained, then the piecewise linearization of Equations (12c) and (12d) is performed with the approach described in Section II-A, where $\chi = \Lambda$. An approximation with four segments for each function is considered,

$$f_j(\Lambda), \quad j = 1, 2, \quad (13)$$

where $j = 1, 2$ indicates the approximation of (12c) and (12d), respectively. Hence, $\ell_j = 4$, $j = 1, 2$, and in total 6 discrete auxiliary variables (7) and 6 continuous auxiliary variables (8) have been introduced. However, because of the additional constraints, only 7 discrete variables combinations are feasible. In particular we have approximated (12c) so that $[\delta_1 = 1] \rightarrow [F = 0]$ and $[\delta_1 = 1] \leftrightarrow [\Lambda \leq \hat{\Lambda}]$, in order to have an exact approximation of the force when $i = 0$. In order to enforce constraints (3) and (4) as output constraints, an output equation

$$y(k) = Cx(k), \quad C = \begin{bmatrix} 1 & 0 & 0 \\ G & 1 & 0 \\ -G & 1 & 0 \end{bmatrix}, \quad (14)$$

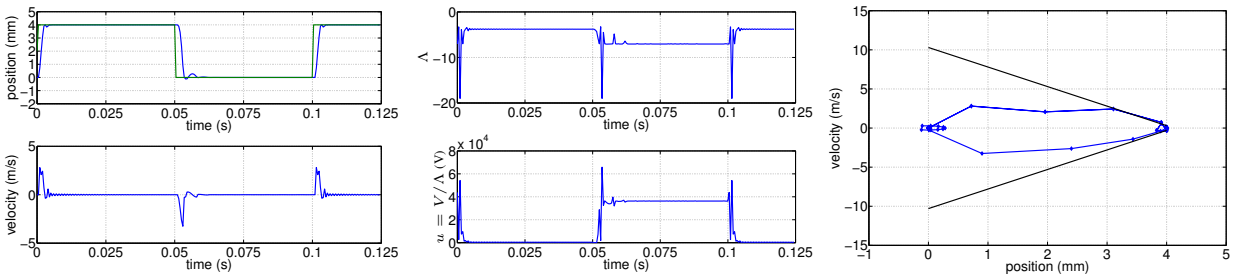

(a) Mechanical subsystem trajectory (b) Electromagnetic subsystem trajectory (c) Mechanical subsystem phase plane

Fig. 2. Coupled hybrid model predictive control results.

is defined, where the first output is the mass position, while the second and the third outputs are useful for defining the soft landing constraint (4) as an output constraint.

Equations (12a), (12b) discretized in time, the linearization (13) of (12c) and (12d), and equation (14) are modelled in HYSDEL and automatically converted into an MLD system with state vector $x^1 = [x\ \dot{x}\ \Lambda]^T \in \mathbb{R}^3$, input $u \in \mathbb{R}$, output $y \in \mathbb{R}^3$, and 12 $(6+6)$ auxiliary variables used for the piecewise linear approximations.

B. Coupled controller simulations

The hybrid MPC optimization problem is formulated as

$$\min_{\{u_k\}_{k=0}^{N-1}} (x(N)-r_x)^T Q_N (x(N)-r_x) + \sum_{k=0}^{N-1} (x(k)-r_x)^T Q_x (x(k)-r_x) + u(k) Q_u u(k) \quad (15a)$$

subject to MLD dynamics (10), (15b)

$$y_{\min} \le y(k) \le y_{\max},\ k = 1 \dots N, \quad (15c)$$

$$u_{\min} \le u(k) \le u_{\max},\ k = 0 \dots N-1\ , \quad (15d)$$

where (15b) is the MLD system computed in Section III-A that approximates (12), (15c) models (3) and (4), and (15d) denotes the range of u. For this hybrid MPC controller, the prediction horizon is $N = 3$, the cost matrices and the input/output bounds are

$$Q_x = Q_N = \begin{bmatrix} 2\cdot 10^{10} & 0 & 0 \\ 0 & 5 & 0 \\ 0 & 0 & 1 \end{bmatrix},\ Q_u = 10^{-8},$$
$$y_{\min} = \begin{bmatrix} -4\cdot 10^{-3} \\ -\infty \\ -10.2 \end{bmatrix},\ y_{\max} = \begin{bmatrix} 4\cdot 10^{-3} \\ 10.2 \\ +\infty \end{bmatrix},$$
$$u_{\min} = -\infty,\ u_{\max} = \infty.$$

Note that the input constraint (6), does not need to be explicitly enforced in (15), since it is already enforced as a hard constraint embedded in the MLD model by the piecewise affine approximation of (12d). Output Constraints are enforced as soft constraints[2]. The vector r_x is the reference vector that the state trajectory shall track. The first component is the external reference mass trajectory, while the second component, for the mass velocity, is constantly 0. The third components is constantly set to Λ_0, so that $\Lambda - \Lambda_0$ is weighted in the cost function. By setting $\Lambda_0 = \hat{\Lambda}$ a null cost is associated with the situation in which the force in the approximated model is null.

Figure 2 reports the nominal results obtained for the coupled MPC approach. The tracking performance ($\mathcal{E}_{\text{cMPC}} = 149.4$) and the mechanical subsystem trajectories are reported in Figure 2(a), while Figure 2(b) shows the trajectories of the electromagnetic subsystem and the input profile. The higher performance with respect to the one obtained in [7] is due to the fact that the whole system is optimized. The peaks of the input signal u occur when Λ reaches large negative values. This depends on the fact that $u \le \frac{V}{\lambda_0 e^{\Lambda}}$ and for $\Lambda \to -\infty$, u becomes unbounded. In Figure 2(c) the phase plane behavior of the mechanical subsystem is illustrated. The soft landing constraints (4) are slightly violated (they are soft constraints). This occurs mainly because of the delay between the actuation of a command and the effects of the command on the state variables, that is comparable with the prediction horizon. However, the violation is small, because of the large cost associated with the soft constraint violations.

In our preliminary tests, the explicit solution of the coupled MPC controller has about 11000 regions, while the hybrid controller evaluated in [7] has about 650 regions. As a consequence, even if the performance obtained is substantially higher, it may be too computationally expensive to implement such a controller.

IV. Decoupled Model Predictive Control

Due to the high complexity of the approach proposed in Section III, that may render it unfeasible for implementation in standard automotive microcontrollers, we consider here the implementation of the decoupled MPC strategy, based on the feasibility study in [7]. We consider an inner-outer control strategy in which the electrical subsystem is controlled by an inner-loop controller. If the inner-loop closed-loop dynamics are much faster than the mechanical subsystem dynamics, the MPC controller can be designed based on the reduced system model,

$$\ddot{x} = -\frac{c}{m}\dot{x} - \frac{k}{m}x + \frac{F}{m}, \quad (16)$$

[1]We use the same symbol (x) for the state vector and the position of the mass. The meaning of such symbol is always clear from the context.

[2]In this paper the constraint $Aw \le b$ is softened as $Aw \le b + \varepsilon \mathbf{1}$, where $\mathbf{1}$ is the vector consisting of all 1. The constraint violation penalty $\rho \cdot \varepsilon^2$, is added in the cost function where the weight ρ is to be two orders of magnitude higher than the higher weight in the objective function.

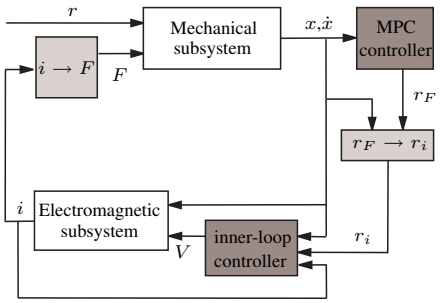

Fig. 3. Controller architecture for the decoupled MPC design

along with constraints (3), (4), (5b) and

$$F \leq k_a \frac{i_{\max}^2}{(k_d + k_b - x)^2}, \tag{17}$$

which defines an upper bound on the available force, related to the maximum available current. The value $i_{\max}$ is computed from equation (1b) in static conditions, considering the maximum voltage $V_{\max}$ in (6). Note that (17) is non-convex, being the hypograph of a convex function.

We consider the control system whose architecture is reported in Figure 3, structured as follows.

- The MPC receives measurements from the mechanical subsystem (16), and generates the force profile r_F for optimally tracking the mass position reference r.
- r_F is converted into a reference current profile (r_i), which is sent as a reference to the electromagnetic subsystem in closed-loop with the inner-loop controller.
- The inner-loop controller actuates the voltage V to make the electromagnetic subsystem track r_i.
- The closed-loop electromagnetic subsystem tracks r_i generating the desired current i.
- The current generates the force F that tracks r_F, and that makes the mass track r.

In the block diagram depicted in Figure 3, the white blocks represent the dynamical subsystems, and the dark grey blocks represent the controllers. The light gray blocks represent the static blocks which act as interfaces. The $r_F \rightarrow r_i$ block converts the force reference into the current reference by inverting Equation (1d). The $i \rightarrow F$ block represents the transduction of the current into the magnetic force acting on the mass computed by Equation (1d).

In the decoupled approach the MPC controller acts as a reference governor for the inner-loop controller, which has the aim of actuating the force indicated by the MPC. Obviously, there is a tracking error related to the inner-loop controller dynamics, because of the time required to reach the desired value of i. If the electrical dynamics imposed by the inner-loop controller are fast with respect to the mechanical dynamics, the effect of such an error is limited and the performance is only slightly degraded with respect to the nominal MPC behavior.

A. Inner-loop controller

The current dynamics, defined by (1b) and (1c), are

$$\frac{di}{dt} = \frac{k_b + z}{2k_a} V - \frac{k_b + z}{2k_a} Ri + \frac{1}{k_b + z} i \frac{dz}{dt}. \tag{18}$$

The simplest way to control such nonlinear dynamics is to design an inner-loop controller $V = g\left(i, z, \frac{dz}{dt}, r_i\right)$ via feedback linearization. Let $\frac{di}{dt} = f(i, z, \frac{dz}{dt}, V)$, we impose that $\frac{di}{dt} = f(i, z, \frac{dz}{dt}, g\left(i, z, \frac{dz}{dt}, r_i\right)) = -\beta i + \gamma r_i$, $\beta, \gamma > 0$. When in closed-loop with the feedback linearization controller, the current dynamics are first-order with a stable pole $p_i = -\beta$ and steady-state gain $\frac{\gamma}{\beta}$.

For the current dynamics (18), the feedback linearization controller is defined by the law

$$V = \frac{2k_a}{k_b + z} \left[\frac{k_b + z}{2k_a} Ri - \frac{1}{k_b + z} i \frac{dz}{dt} - \beta i + \gamma r_i \right], \tag{19}$$

where the reference r_i is obtained from the force reference r_F, produced by the MPC controller, by inverting Equation (1d). In the decoupled MPC design, the effects of the mass position and velocity on the electromagnetic subsystem are treated as disturbances, thus, they must be much slower than the electromagnetic subsystem dynamics. Moreover, if the dynamics imposed by the feedback linearization controller are too slow, large constraint violations and instability may occur.

A drawback of the feedback linearization controller is that the voltage command can take large values and vary rapidly, and that small modelling errors can cause loss of stability or performance degradation. The main concerns here are the properties of the decoupled MPC design, hence we use controller (19) for simplicity, while noting that alternatives, more robust design can be used.

B. Hybrid decoupled MPC

In this model predictive controller the electrical dynamics are disregarded, but the force is limited by the maximum available current through force constraint (17). The state vector is $x = \left[\begin{smallmatrix} x_1 \\ x_2 \end{smallmatrix}\right] \in \mathbb{R}^2$, where x_1 and x_2 are the position and the velocity of the mass, respectively, and the input $u \in \mathbb{R}$ is the applied force. Constraint (17) is nonlinear and defines a nonconvex set, the hypograph of a convex function. The hybridization technique described in Section II-A can be applied to obtain a piecewise affine approximation of such a constraint, and it ensures that (17) is satisfied without being excessively conservative.

We have considered a piecewise affine approximation with three segments ($\ell = 3$), and as a consequence, 2 Boolean and 2 real auxiliary variables have been introduced. After applying the technique described in Section II-A, the force constraint (17) is defined as

$$u \leq z_1 + z_2, \tag{20}$$

where z_1 and z_2 are defined by (7) and (8) with $\chi = x_1$ and $\ell = 3$. Clearly, $f(x_1) = z_1 + z_2$ is the function that approximates the right-hand side of (17). Model (16) with (7), (8), (20), and the output equation $y(k) = \left[\begin{smallmatrix} 1 & G & -G \\ 0 & 1 & 1 \end{smallmatrix}\right]^T x(k)$ can

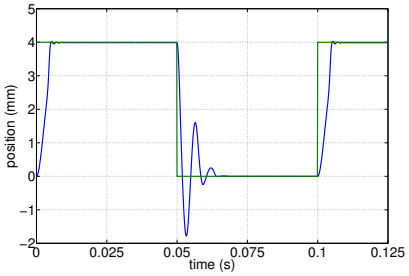

(a) tracking performance

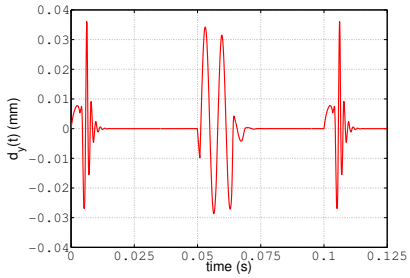

(b) position difference $d_y(t)$

Fig. 4. Decoupled hybrid MPC of the mass-spring-damper system.

be modelled in HYSDEL, and the equivalent Mixed Logical Dynamical (MLD) hybrid model corresponding to the saturated magnetic actuator is obtained. Using this model for prediction, the hybrid MPC optimization problem (15) can be formulated, where now $x \in \mathbb{R}^2$ and $Q_x = Q_N = \left[\begin{smallmatrix} 2\cdot 10^6 & 0 \\ 0 & 0 \end{smallmatrix}\right]$, $Q_u = 10^{-7}$, $N = 3$. Output constraints, where $y_{\min}$ and $y_{\max}$ are the same as for problem (15), and input constraints, where $u_{\min} = 0$ and $u_{\max} = +\infty$, are enforced as soft constraints, while the approximation of (17) is enforced as a hard constraint, and embedded into the MLD model.

C. Simulation of the decoupled MPC

We have tested the decoupled linear/hybrid MPC approach, and we have compared the results with the ones obtained in the ideal case, in which the dynamics of the electromagnetic subsystem are infinitely fast.

We have designed the inner-loop controller (19) with $\beta = \gamma = 1.5 \cdot 10^5$. Since the mechanical subsystem is a second order system with damped resonance $\omega_r = 950$ rad/s and 3db-bandwidth $BW_3 = 3 \cdot 10^3$ rad/s, the feedback linearization controller imposes current dynamics ($BW_3 = 1.5 \cdot 10^5$ rad/s) much faster than the mechanical ones. The decoupled controller architecture and the nonlinear system (1) have been implemented in SIMULINK. The position reference is a square wave between the critical value 4 mm and 0 mm and frequency 10 Hz, the same used in Section III-B. The initial state is $x_0 = [0\ 0]^T$.

Figure 4 reports the results obtained with the decoupled hybrid MPC controller, with (19) as inner-loop controller.

In Figure 4(a) the mass trajectory (solid) when tracking the reference (dashed) is shown, and $\mathcal{E}_{\text{dhMPC}} = 237$. Figure 4(b) reports the difference $d_y(t) = y_1(t) - y_1^{(MPC)}(t)$, where y_1 is the position obtained by the decoupled hybrid MPC, in which the current dynamics are imposed by the feedback linearization controller, while $y_1^{(MPC)}$ is the nominal MPC position, assuming infinitely fast current dynamics. The difference is very small, because of the fast response of the controlled current dynamics. Note that the constraints are slightly violated: this is mainly due to the current dynamics and only for a limited amount due to the soft constraints in the optimization problem.

The average CPU time on a Pentium-M 2 GHz with 1 GB RAM, Cplex 9 and MATLAB 7 for simulating the implicit decoupled hybrid MPC in closed-loop with the nonlinear system (2) and the inner-loop controller (19) is 6.5 sec. In the same computer, the execution cycle of the C-code implementation of the explicit hybrid decoupled MPC takes 0.025 ms in average, and 0.3 ms in the worst case.

V. CONCLUSIONS

We have presented different MPC strategies to control magnetic actuators which are common components of automotive systems. First, a strategy based on the complete system model has been presented. Then, we have implemented a controller architecture where the controllers for the mechanical and electromagnetic subsystems are decoupled, and the MPC controller optimizes only the mechanical subsystem behavior. The performance of the decoupled control scheme is lower, but still satisfactory, and the complexity of the controller is reduced.

REFERENCES

[1] D. Hrovat, J. Asgari, and M. Fodor, "Automotive mechatronic systems," in *Mechatronic Systems, Techniques and Applications: Volume 2–Transportation and Vehicle Systems*. Gordon and Breach Science Publishers, 2000, pp. 1–98.

[2] M. Barron and W. Powers, "The role of electronic controls for future automotive mechatronic systems," *IEEE/ASME Transactions on Mechatronics*, vol. 1, no. 1, pp. 80–88, June 1996.

[3] L. Guzzella and A. Sciarretta, *Vehicle Propulsion Systems: Introduction to Modeling and Optimization*. Springer Verlag, 2005.

[4] S. Qin and T. Badgwell, "A survey of industrial model predictive control technology," *Control Engineering Practice*, vol. 93, no. 316, pp. 733–764, 2003.

[5] J. Maciejowski, *Predictive control with constraints*. Englewood Cliffs, NJ: Prentice Hall., 2002.

[6] A. Bemporad, M. Morari, V. Dua, and E. Pistikopoulos, "The explicit linear quadratic regulator for constrained systems," *Automatica*, vol. 38, no. 1, pp. 3–20, 2002.

[7] S. Di Cairano, A. Bemporad, I. Kolmanovsky, and H. Hrovat, "Model predictive control of nonlinear mechatronic systems: An application to a magnetically actuated mass spring damper," in *2nd IFAC–Analysis and Design of Hybrid Systems*, 2006.

[8] E. Sontag, "Nonlinear regulation: The piecewise linear approach," *IEEE Trans. Automatic Control*, vol. 26, no. 2, pp. 346–358, April 1981.

[9] W. Heemels, B. de Schutter, and A. Bemporad, "Equivalence of hybrid dynamical models," *Automatica*, vol. 37, no. 7, pp. 1085–1091, July 2001.

[10] F. Torrisi and A. Bemporad, "HYSDEL — A tool for generating computational hybrid models," *IEEE Trans. Contr. Systems Technology*, vol. 12, no. 2, pp. 235–249, Mar. 2004.

[11] A. Bemporad, *Hybrid Toolbox – User's Guide*, Dec. 2003, http://www.dii.unisi.it/hybrid/toolbox.

[12] A. Bemporad and M. Morari, "Control of systems integrating logic, dynamics, and constraints," *Automatica*, vol. 35, no. 3, pp. 407–427, 1999.

[13] C. A. Floudas, *Nonlinear and Mixed-Integer Optimization*. Oxford University Press, 1995.